HO CHI MINH CITY UNIVERSITY OF TECHNOLOGY

FACULTY OF MECHANICAL ENGINEERING

DEPARTMENT OF MECHATRONIC ENGINEERING

FINAL YEAR PROJECT REPORT

DESIGN OF AN AUTOMATED SCREWING MACHINE FOR A REAR HUB OF A BICYCLE

Student:

Võ Đức Trí 1513682

Supervised by:

Assoc. Prof. Nguyễn Quốc Chí

HO CHI MINH CITY, 2020

ABSTRACT

Covid-19 pandemic has bad effects on the global economic. Due to the labor shortage, more and more factory wants to automate their producing lines. This thesis proposes a solution for an automated nut running system for the back-wheel assembly of bicycles using robotic arm and computer vision. The heart of this system is the nut position determination algorithm which is proposed and carefully examined.

TABLE OF CONTENTS

LIST OF FIGURES

LIST OF TABLES

CHAPTER 1. INTRODUCTION

1.1 Motivation

The Covid-19 pandemic made more than one third of the world's population placed on lockdown, which led to the global economic crisis. Vietnam, which has managed to contain the pandemic by preventing rather than fighting the Covid-19, also suffers a slight economic recession.

SMEs (Small and medium-sized enterprises) are one of the first victims of the pandemic. Quarantine and lock-down make them to stop the production lines and then causes some declines in revenue and net profit. Factory automation seems to be the key to this problem. Less people in the workplace will lower the risk of virus spread-out.

This report proposes a solution for an automated nut running system for the back-wheel assembly of bicycles using robotic arm and computer vision. Figure 1.1 shows an example of bicycle assembly line.

Figure 1.1 An example of bicycle assembly line.

1.2 Design Objective and Scope

1.2.1 Objective

Design an automated nut running system for the back-wheel assembly of bicycles using robotic arm and computer vision.

1.2.2 Scope

The system must be applicable for bicycles with following specifications:

- Frame style: Diamon Frame.
- Bicycle dimensions (Figure 1.2)
- Shaft: in black or silver and has M-10 thread.
- Nuts: in silver, ISO 4161 M-10 type (Figure 1.2).
- Tightening force: 46 Nm.
- Shaft's maximum rotating angles: $\theta_{X_X} = 3.5^o, \theta_{Z_X} = 0.65^o$ (Figure 1.2).
- Bicycle's weight: 10 kg.
- The nuts should be ran close enough to hold the kickstands (if any).

The system also has to meet the following requirements:

- The nuts must be tightening at such positions that the wheel is centered with respect to the bike's frame and the chain drive is tensioned.
- Nut running productivity: 30 bikes per hour.
- Head to a fully automated bicycle assembly system.

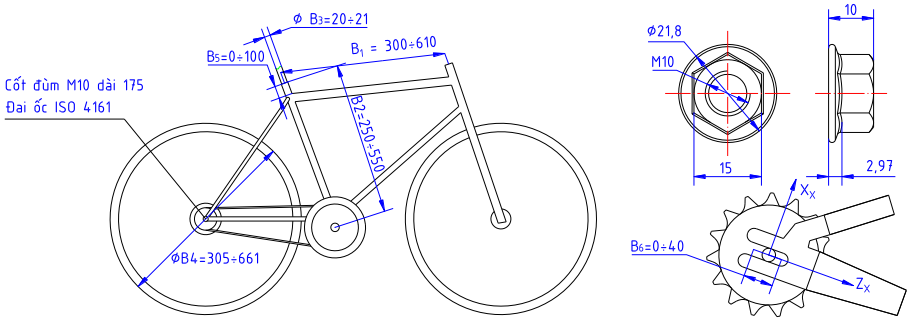

Figure 1.2 Bicycle's basic dimensions

OK NG

Figure 1.3 Illustration of OK and NG products.

1.3 Report Organization

After having identified the design objective and scope in Chapter 1, the system design will be described in Chapter 2. Then, Chapter 3 shows the experiment setup and its results with some discussions. Finally, the conclusion and future work are mentioned in Chapter 4.

CHAPTER 2. SYSTEM DESIGN

2.1 Overview

This section describes briefly the working principle of the system. The workspace organization is shown in Figure 2.1. There are two main parts should be notice here: the mounting cart and the robot's tool. The reason why "cart" instead of fixtures is that after the nuts have been tightening, the cart is then moved to another place to continue assembling other components. In case of using fixtures, lead time is increased when the bike is move to the ongoing period.

Another notice is that although this system can work with 3 carts, all the algorithm later will be described in case of 1 cart, for simplicity.

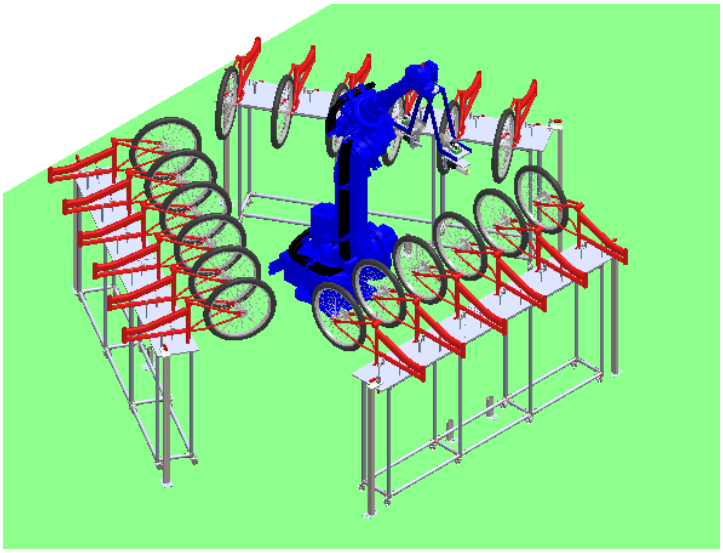

Figure 2.1 Workspace organization.

The working principle of the system is described step-by-step in Figure 2.2.

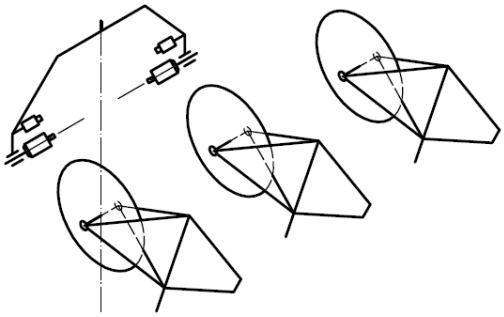

(a) Robot is at the prepare position for station i. .

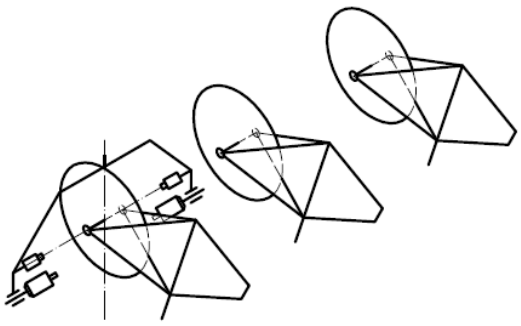

(b) Robot moves to the capture position for station i.

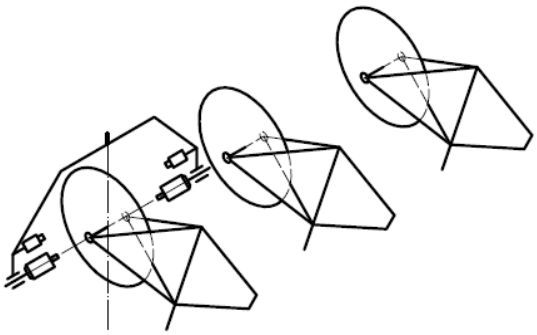

(c) After the image is processed robot moves to the nut-holding-position. Then, the linear cylinders extract and hold the nut.

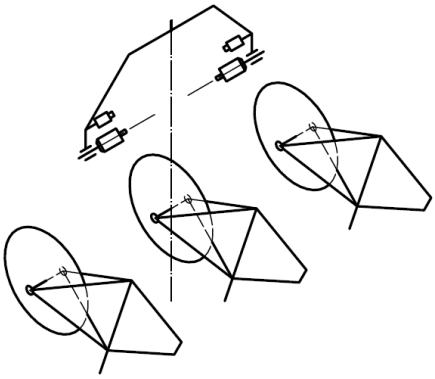

(d) Robot moves to the proper nut-running position. Then, the motors are activated and start to tighten the nuts.

Figure 2.2 Working principle of the system.

2.2 Nuts' Pose Estimation Algorithm

2.2.1 Capture and Nut-running Positions

The capture and nut-running positions, $\mathbf{P_{capture-i}}$ and $\mathbf{P_{run-i}}$ is determined based on the mechanical drawing of the bicycle by (2.1-2.3), as illustrated in Figure 2.3. Following the mechanical design of the mounting cart (section 2.4.2), the station translational vector should be $\mathbf{t_{stations}} = [0 \quad 500 \quad 0]^T$.

$$\mathbf{P_{capture-i}} = \mathbf{P_{ref-i}} + \mathbf{\Delta P_{capture-X}} \tag{2.1}$$

$$\mathbf{P_{run-i}} = \mathbf{P_{ref-i}} + \mathbf{\Delta P_{run-X}} \tag{2.2}$$

$$\mathbf{P_{ref-i}} = (\mathbf{i} - \mathbf{1})\mathbf{t_{stations}} \tag{2.3}$$

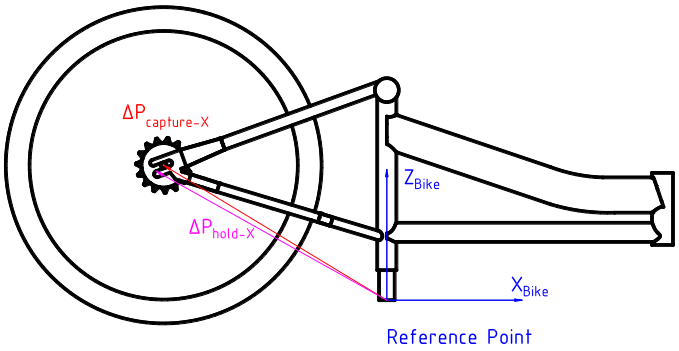

Figure 2.3 Bicycle's mechanical drawing.

2.2.2 Nut-holding Position

The nut-holding position is determined based on the variation of the nut's position in the current images with respect to a pre-defined zero-position. The zero-position is defined as the position at which the shaft, and the camera lens is coaxial. Let denote this position as $\mathbf{P_0}$ (robot position) and the corresponding nuts center positions in two images are $\mathbf{p_{01}}$ and $\mathbf{p_{02}}$. From $\mathbf{P_0}$, control the robot to move to position $\mathbf{P_1}$ at which the shaft and the nut-runner sockets are coaxial. Now the translational vector between the camera coordination and the sockets coordination is define as $\mathbf{t} = \mathbf{P_1} - \mathbf{P_0}$. The nut-holding position is shown in. The variation vector $\mathbf{\Delta P}$ will be determine in 2.2.4.

$$\mathbf{P_{hold}} = \mathbf{P_{capture-i}} + \mathbf{t} + \mathbf{\Delta P} \tag{2.4}$$

$$\mathbf{\Delta P} = [\Delta X_1 \quad 0 \quad \Delta Z_1 \quad \beta \quad 0 \quad \alpha]^T \tag{2.5}$$

Note that the center of rotation must be placed at the expected nut's position to reduce calculations.

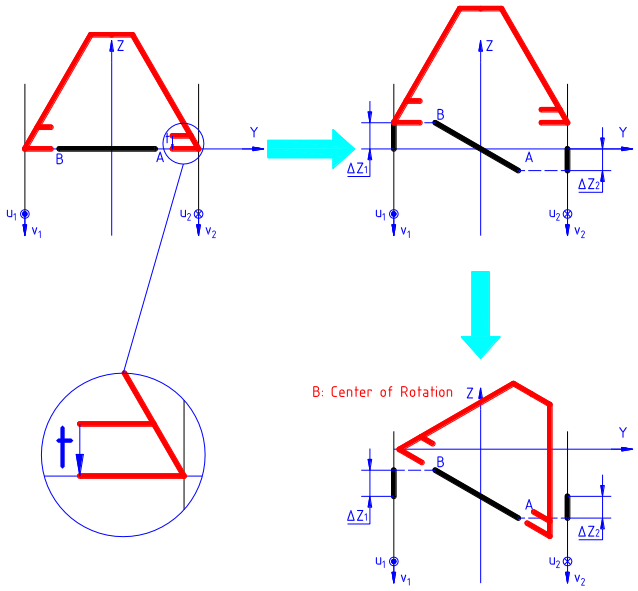

Figure 2.4 Nut-holding process illustration.

2.2.3 Nut's Center in Image Determination

Figure 2.5 gives the main algorithm for the nut's center in image determination. This algorithm is illustrated step by step in Figure 2.6.

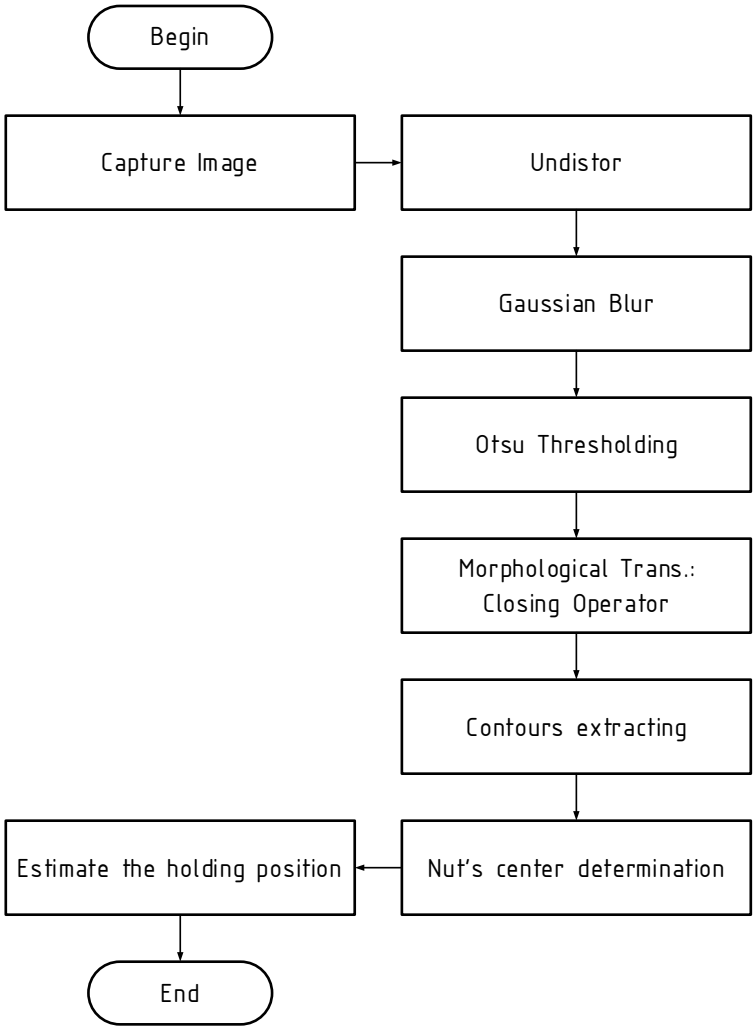

Figure 2.5 Algorithm for the nut center in image determination.

(a) Origin Image.

(b) Undistorted.

(c) Gaussian Blurred

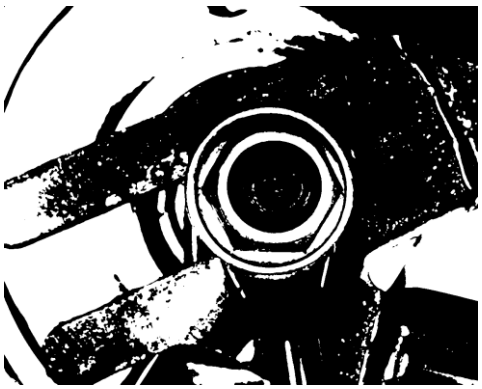

(d) Otsu's Thresholded

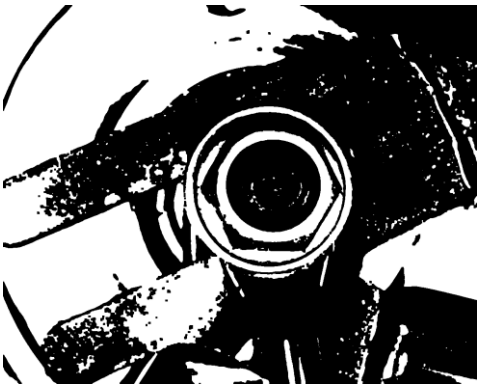

(e) Closing Transformed

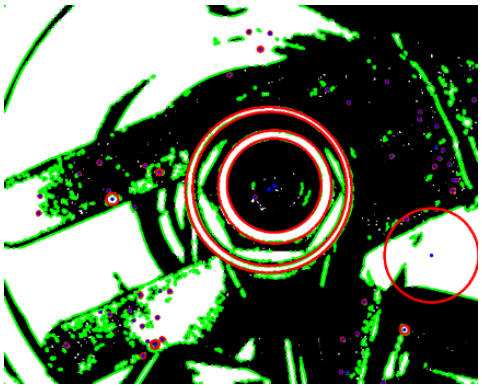

(f) Contour Extracted [1]

Figure 2.6 Illustration of the nut-holding position determination algorithm (up to the contour extraction step).

After having extracted all contours from the image, the next step is looking for the appropriate circle among these contours and calculate its center. The criterion is that the min-fitting-circle of the contour has the similar area w.r.t the contour area and its radius is similar to the expected value calculated based on the real nut size. This algorithm is shown in Figure 2.7.

The nut's center is calculated using image moments, which is shown in (2.6) to (2.8).

$$m_{ij} = \sum_{u,v} I(u,v) \cdot u^i \cdot v^j \tag{2.6}$$

$$A = m_{00} \tag{2.7}$$

$$\bar{u} = \frac{m_{10}}{m_{00}}, \qquad \bar{v} = \frac{m_{01}}{m_{00}} \tag{2.8}$$

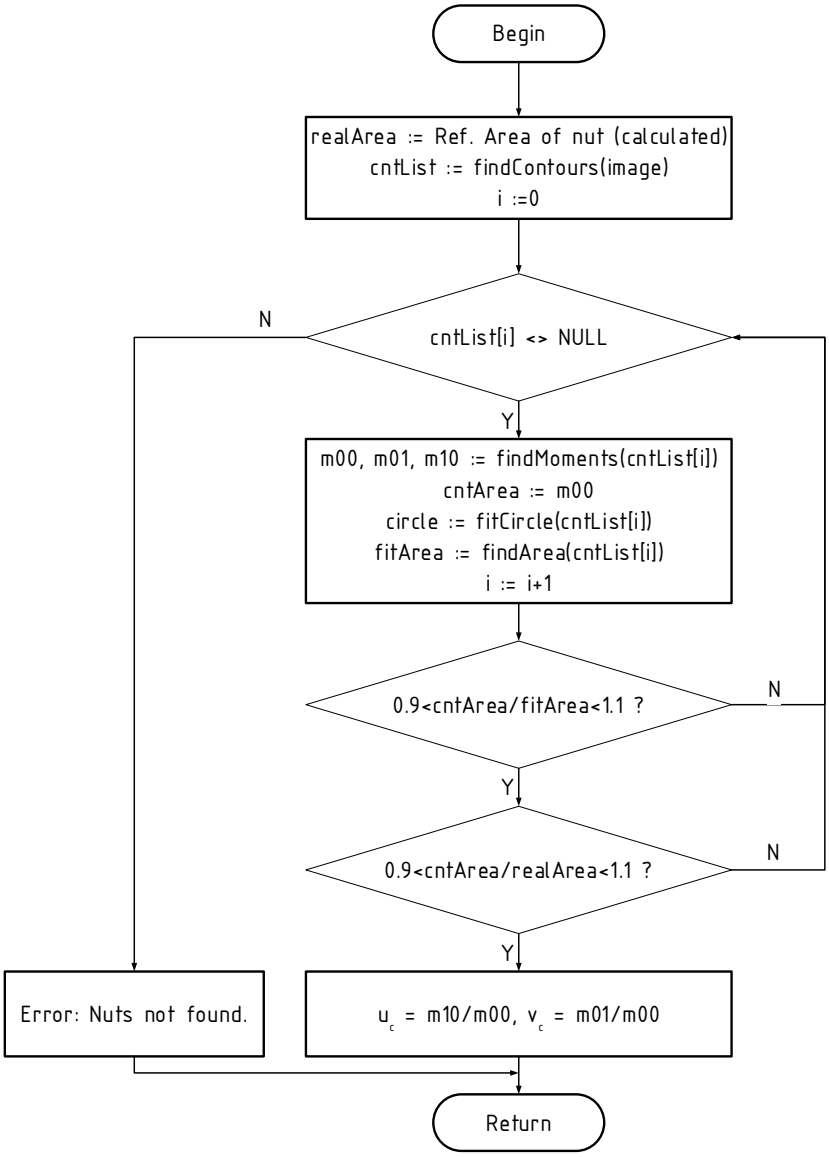

Figure 2.7 Nut center in image determination algorithm.

2.2.4 Variation Vector Determination

Undistorted images can be sent to the pin-hole model to estimate the corresponding 3D position of a point on an image. When the object and image planes are ideally parallel, this relation can be described as (2.9) and (2.10). Note that Δu_1 defines the variation of the current center w.r.t the 0-position along the u-axis in the image.

$$\Delta X_1 = r_{11}\Delta u_1, \qquad \Delta Z_1 = -r_{21}\Delta v_1 \tag{2.9}$$

$$\Delta X_2 = -r_{21}\Delta u_2, \qquad \Delta Z_2 = -r_{22}\Delta v_2 \tag{2.10}$$

Using the model shown in Figure 2.8, the estimated rotating angles are given in (2.11)-(2.13).

$$AB = \sqrt{MN^2 - (\Delta Z_1 - \Delta Z_2)^2} = \sqrt{L^2 - (\Delta Z_1 - \Delta Z_2)^2} \tag{2.11}$$

$$\alpha = \text{asin}\frac{\Delta X_1 - \Delta X_2}{AB} = \text{asin}\frac{\Delta X_1 - \Delta X_2}{\sqrt{L^2 - (\Delta Z_1 - \Delta Z_2)^2}} \tag{2.12}$$

$$\beta = \text{asin}\frac{\Delta Z_1 - \Delta Z_2}{AB} = \text{asin}\frac{\Delta Z_1 - \Delta Z_2}{\sqrt{L^2 - (\Delta Z_1 - \Delta Z_2)^2}} \tag{2.13}$$

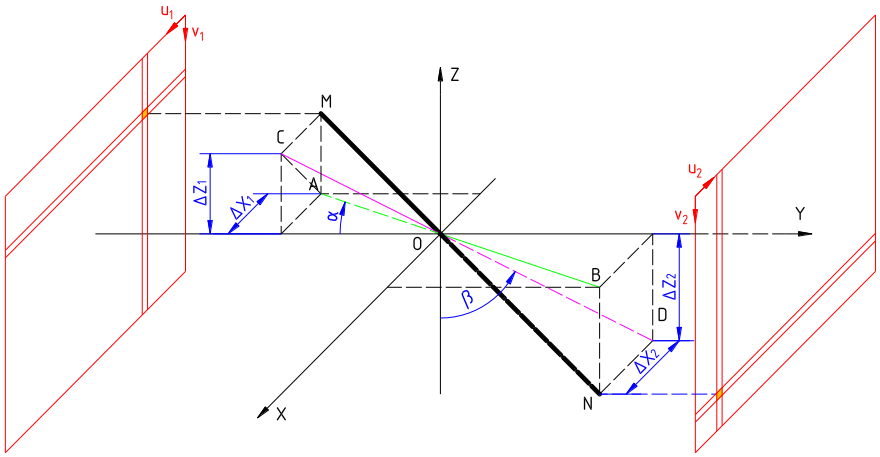

Figure 2.8 Model for calculating rotating angles.

2.2.5 Errors Consideration

The holding condition is given by (2.14) and (2.15). Figure 2.9 gives a calculation model for this condition. Note that in this system, the socket is opened as shown in Figure 2.9.

$$d = \sqrt{2}\left(\left|\Delta\tilde{Z}_1\right| + R_{shaft}\cos\tilde{\beta}\right) \leq R_{safe} \tag{2.14}$$

$$R_{safe} = \frac{12 + 7.5}{2} = 9.75\ mm \tag{2.15}$$

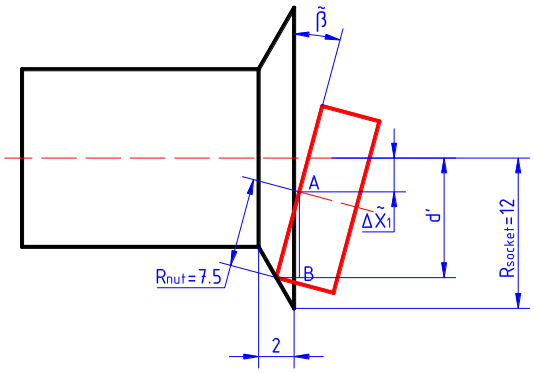

Figure 2.9 Model for considering the holding condition.

The error consideration model is shown in Figure 2.10 from which the estimating values are calculated as shown in (2.16) - (2.19).

$$\Delta Z = \Delta Z_1 - \Delta Z_2 = L_\beta \sin\beta \tag{2.16}$$

$$\Delta\tilde{Z}_1 = -1.1 \cdot 0.5 K_\beta \sin\alpha \tag{2.17}$$

$$\hat{\beta} = \text{asin}\frac{\Delta\hat{Z}_1 - \Delta\hat{Z}_2}{\sqrt{L^2 - \left(\Delta\hat{Z}_1 - \Delta\hat{Z}_2\right)^2}} \tag{2.18}$$

$$L_\beta^2 = L^2 - (\Delta Z)^2 = L^2 - L_\beta^2 \sin^2\beta \Longrightarrow L_\beta = \frac{L}{\sqrt{1 + \sin^2\beta}} \tag{2.19}$$

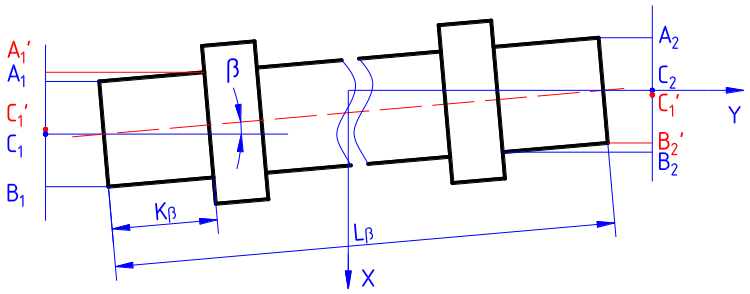

Figure 2.10 Model for error consideration.

The double capture solution is proposed to reduce the angular error. Its effect is shown in Table 2.1. It is simply achieved by moving to the new position returned by the first capture time, then capture again and return the new position as $\mathbf{P_{hold}}$.

Table 2.1 Effect of the double capture solution.

	First Capture	**Second Capture**
L	$170\ mm$	
β	14^o	2.44^o
$\Delta\tilde{Z}_1$	0.45^o	$-0.47\ mm$
$\tilde{\beta}$	2.44^o	0.31^o
d	$10.8\ mm$	$7.73\ mm$

2.3 Auto Tuning for Camera

Lighting may have great effect on the final result of an image processing system, as shown in Figure 2.11. When the lighting of the environment changed, the camera needs to find its new exposure time to continue working normally.

The algorithm for the Auto Tuning function is shown in Figure 2.12.

It is basically a loop that searching for the maximum and minimum proper exposure time, then takes the mean value.

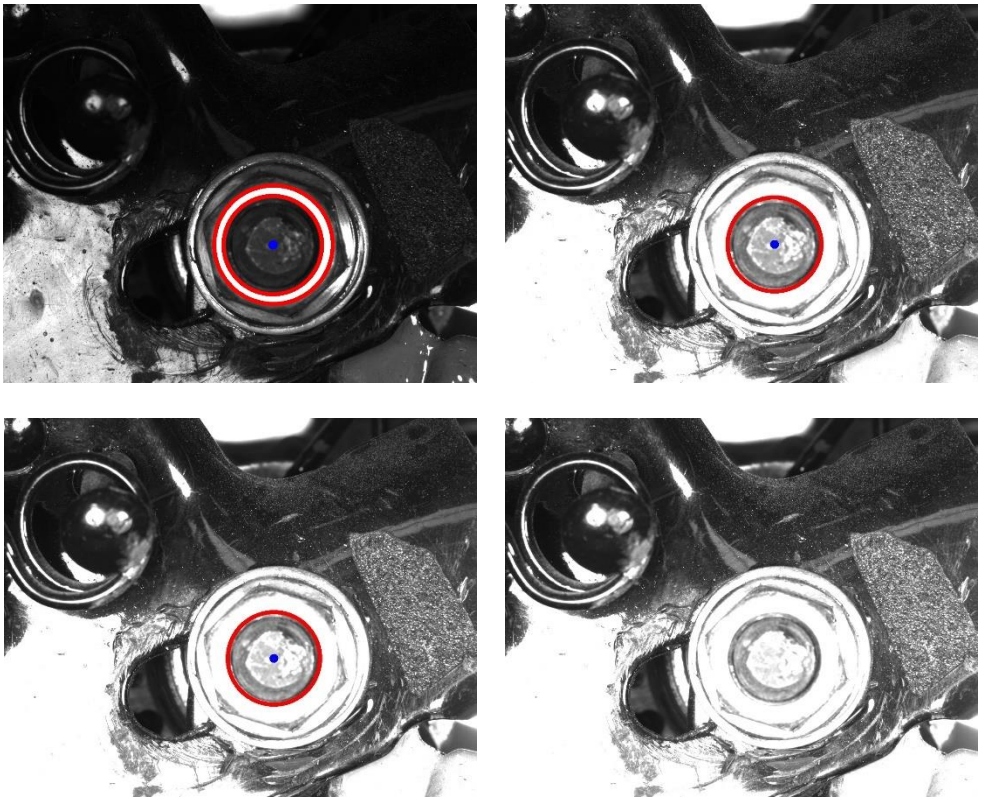

Figure 2.11 Lighting effect on nuts detection.

2.4 Mechanical Design

2.4.1 Robot's Tool

2.4.1.1 Requirements

The robot's tool has to meet the following requirements:

- Ensure the coaxial tolerance of the two nut-running sockets: 0.3 mm.
- Maximum size: 800×1000×300 mm

- Be safety under external forces including reaction moments 46 Nm (when at the end of the tightening period), reaction force of the cylinder and pushing force applied by workers (150 N for each).

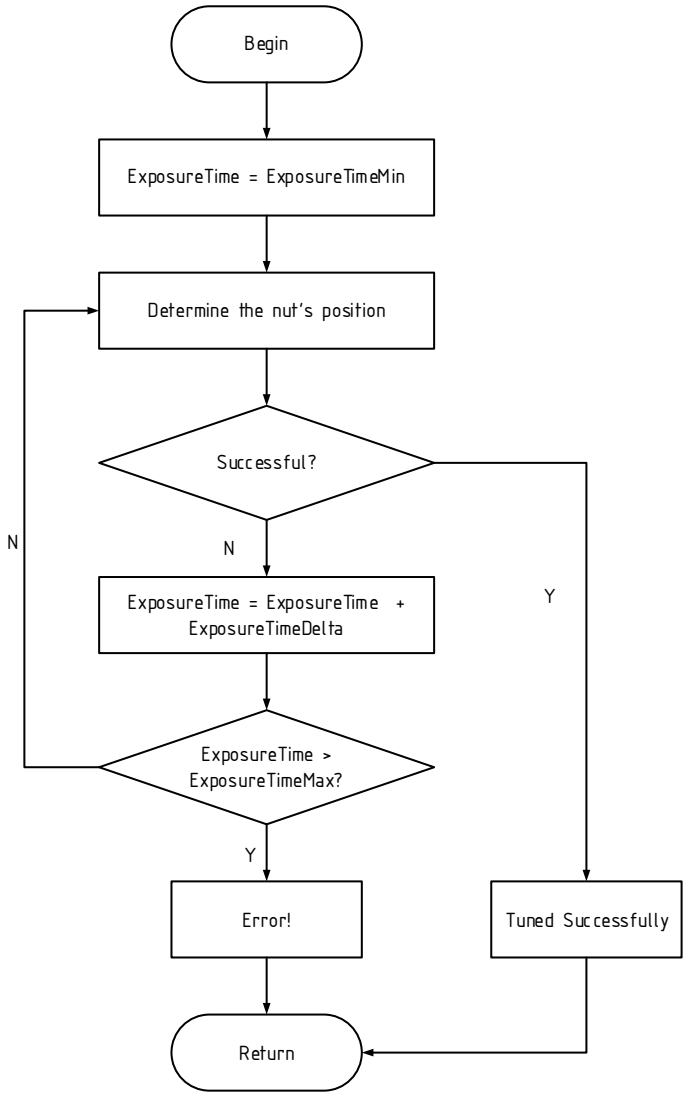

Figure 2.12 Algorithm for the auto tuning algorithm.

2.4.1.2 Robot's Tool Design

The principle diagram of the robot's tool is shown in Figure 2.13. Base on this diagram, the tool's design is shown in Figure 2.14. Note that the wires (pneumatic and electric) should be fixed on the tool to prevent any connection loss. The main frame's minimum factor of safety under static loads is about 1.6, which is shown in Figure 2.15. The devices selection is shown in Table 2.2.

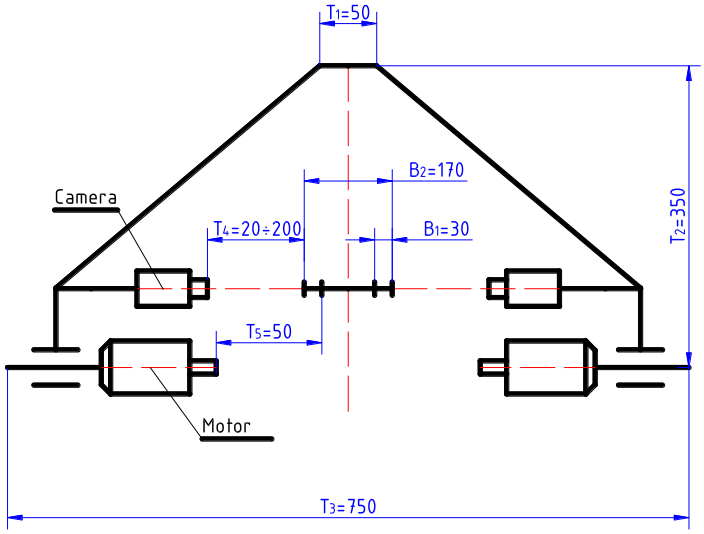

Figure 2.13 Principle diagram of the robot's tool.

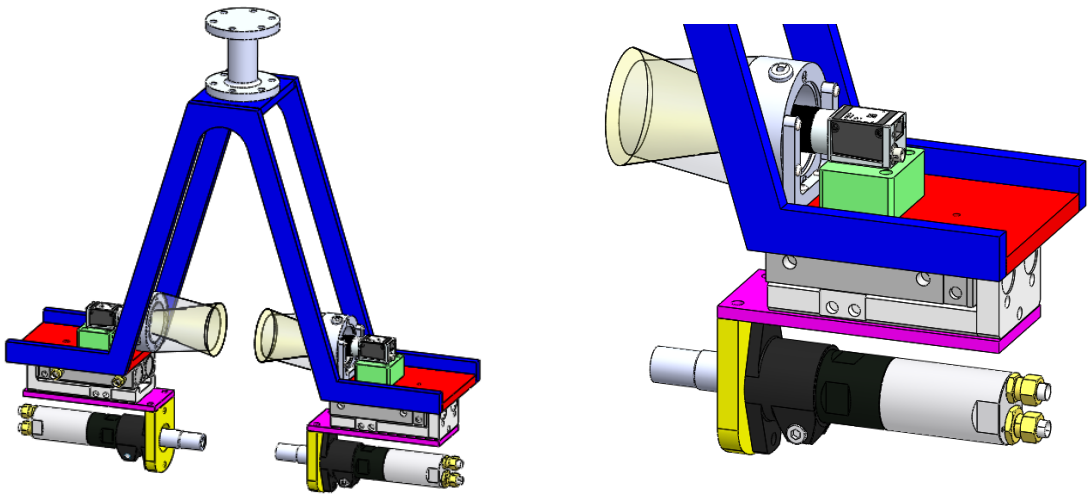

Figure 2.14 Design of robot tool.

Table 2.2 Devices selection for the mechanical design.

Device	**Requirements**	**Selection**
Motor	Tightening force: $46Nm$. Tightening time: $3s$.	LZB42-L-A005-11 (Atlas Copco)
Linear cylinder	Static moment 46 Nm. Working load: $W = 15N$ Min speed: $10mm/s$	MXQ25-50 (SMC)

	Stroke: $50mm$.	
Camera	Min resolution: 800x400 px Industrial standards	
Lens	Capture widows: 60x30. Working distance: <200	C125-0818-5M-P f6mm (Basler)
Lighting	Working distance: 100 Brightness: >5000 lux	RL1424-WHI-100-XXL-24 (Advanced Illumination)

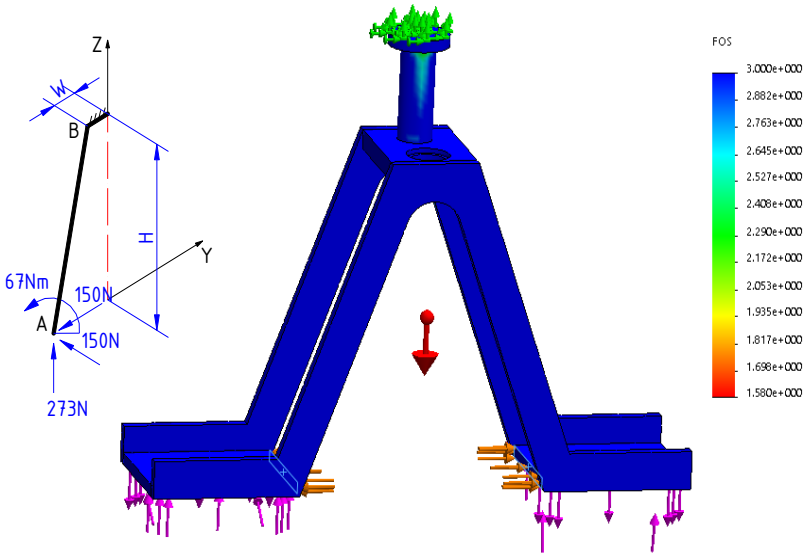

Figure 2.15 Static loads factor of safety calculation for the robot tool using Solidworks.

2.4.2 Mounting Cart

The mounting cart's design is shown in Figure 2.16. The distance between the subassemblies are 500 mm. The mounting, or more clearly, clamping principle is shown in Figure 2.20. Because the cart is moving, all mechanism is manually operated.

One more point should be noticed when designing the cart is that the center of mass of the cart should fall in the region limited by its wheels. That's why the final design of the cart looks like what is shown in Figure 2.18. It is thanks to the two holes at the two ends of the cart that the cart is positioned, as shown in Figure 2.19.

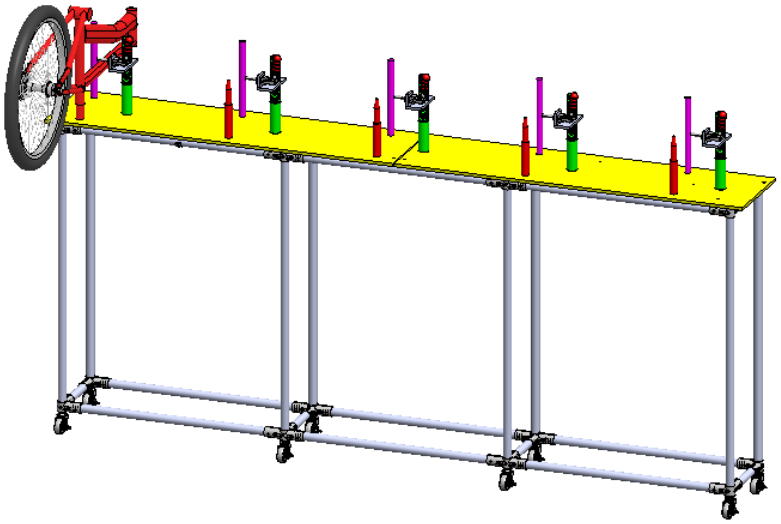

Figure 2.16 Design of the mounting cart.

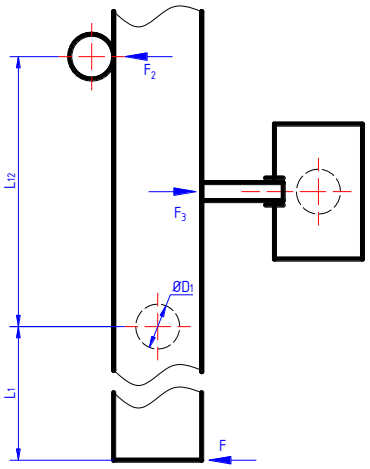

Figure 2.17 Clamping principle of the mounting cart.

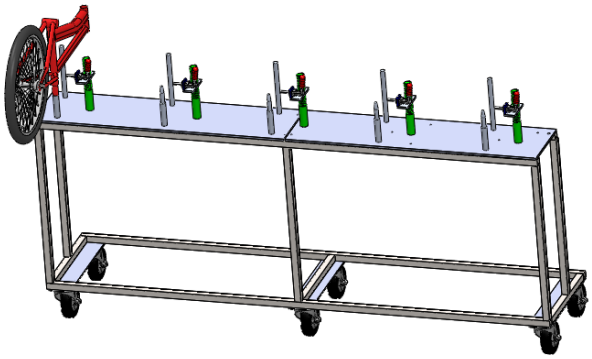

Figure 2.18 Final design of the mounting cart.

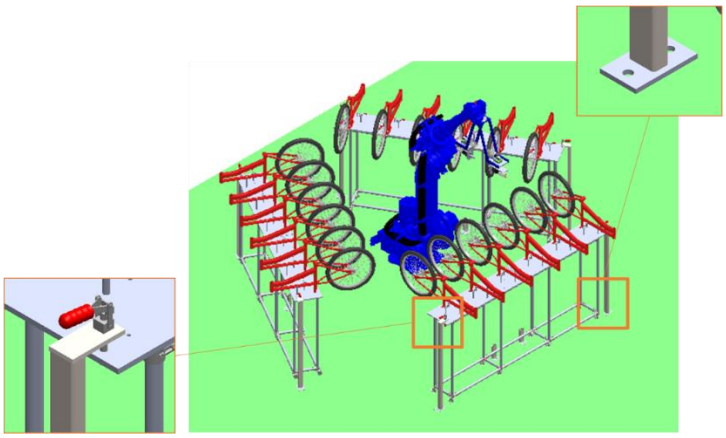

Figure 2.19 Mounting cart positioning with respect to the robot.

2.5 Pneumatic System Design

The principle diagram of the pneumatic system is shown in Figure 2.20. Note that the working pressure of the cylinder and the air motor is different. The robot arm itself has two air lines inside the robot, which can hold maximum 5 bar pressure. The cylinder will use those air lines and the motor, which requires higher pressure and flow rates has to connect to the air source on the ground by attach the tubes along the robot arm.

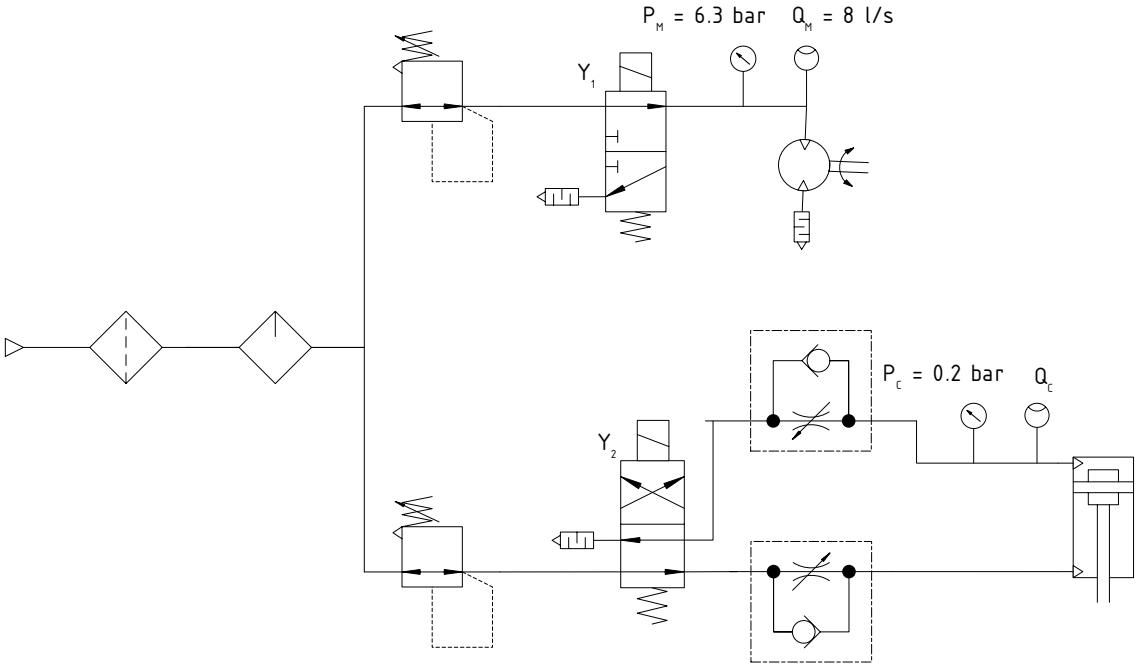

Figure 2.20 Principle diagram of the pneumatic system.

2.6 Electric System Design

2.6.1 Devices selection

The main devices selection is shown in Table 2.3.

Table 2.3 Devices selection for the electric system design.

Device	**Requirements**	**Selection**
Computer	Gigabit Ethernet (RJ45) Avaiable. RAM: 1GB. CPU: 2GHz, multithreading supported. OS supported	IPC-510 (Core i3) (AdvanTech)
PLC	Min: 2 digital inputs and 2 digital outputs Modbus TCP supported	S7-1200 CPU 1211C (Siemens)
HMI	Modbus TCP supported Min resolution: 7”. CPU min speed: 400 MHZ.	MT8071iP (Weintek)
Switch	Minimum 6 ports including: • 2 ports PoE GigE • 2 ports GigE • 2 ports 100Mbps	IPS33064P (ONV)

2.6.2 Devices Communication Organization

All devices support the Ethernet port, so that it is convenient to use MODBUS protocol as the basic communication method between the devices. The connection diagram is shown in Figure 2.21.

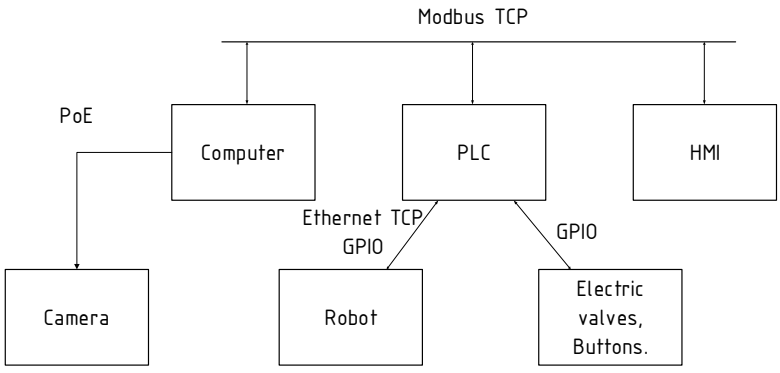

Figure 2.21 Devices communication diagram.

CHAPTER 3. EXPERIMENTS

3.1 Experiment Setup

The experiment is set up to

- examine the stability of the nut-holding position determination algorithm.
- examine the processing time of the nut-holding position determination algorithm.
- examine the working process to find if any risk might occur.

The experiment setup is described in Figure 3.1 to Figure 3.4.

Figure 3.1 Overview of the experiment system.

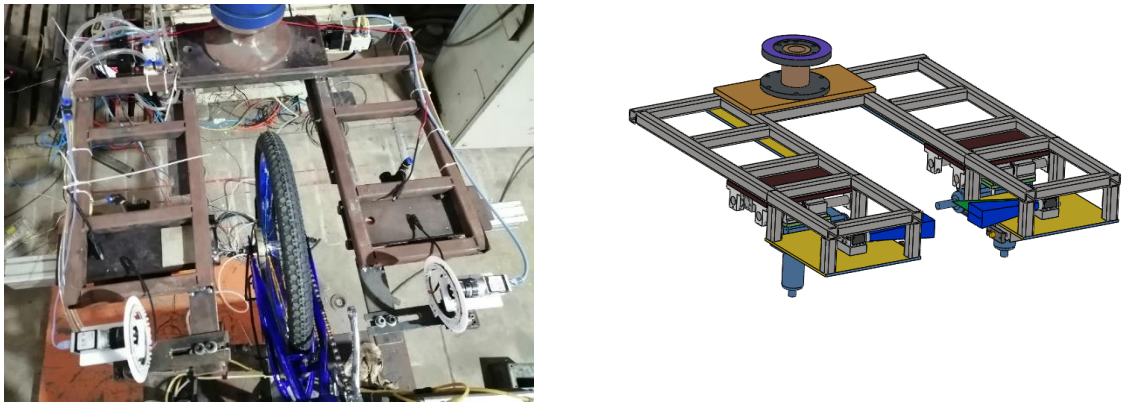

Figure 3.2 Robot tool of the experiment system.

Figure 3.3 In the experiment, the bike is mounted on a fixed fixture.

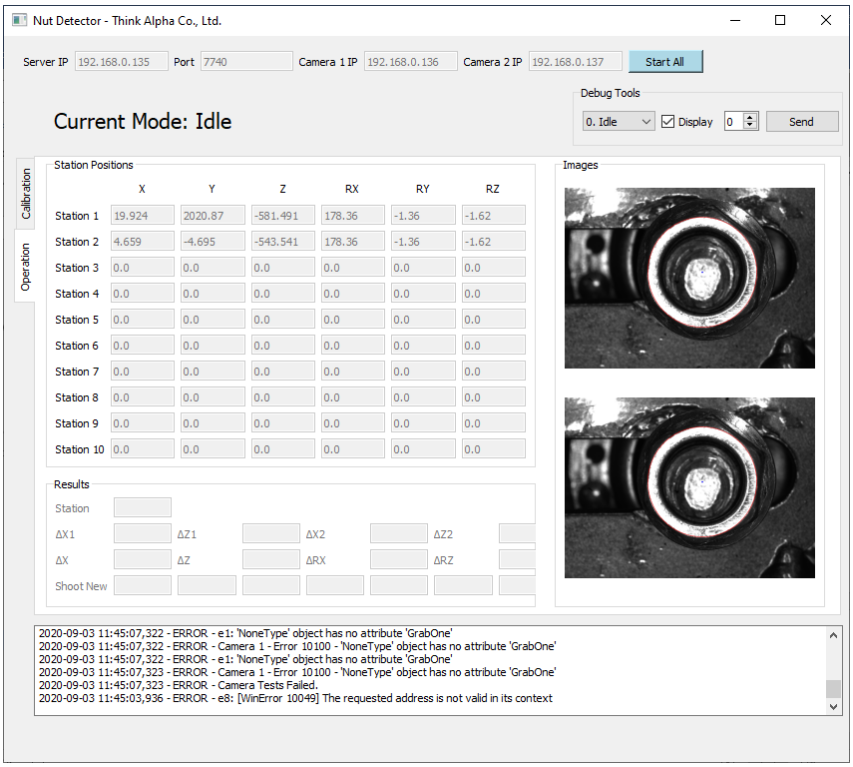

Figure 3.4 Computer program in the experiment.

3.2 Results and Discussion

3.2.1 Algorithm's stability

To examine the Algorithm's stability, let the system run periodically (without turning on the motor and cylinder). Collect the results from 14:51:10 06/07/2020 to 00:13:47 07/07/2020, the data is processed and shown in Table 3.1. The maximum 3σ error is about 0.16 mm, which is acceptable for the system.

Table 3.1 Processed data from experiment.

	X (mm)	**Z (mm)**	**RX (deg)**	**RZ (deg)**
Max	188.309	-348.44	178.653	-3.201
Min	188.124	-349.402	177.848	-3.237
Mean	188.227	-348.557	178.5143	-3.2182
Std. Variation	0.044	0.054	0.034	0.004
3σ	0.132	0.163	0.102	0.012

3.2.2 Algorithm Processing Time

Using Asus K555LB (CPU Intel i5-5200U 2.2GHz) as the computer, the logged processing time is describe as follow:

- In normal operation: 0.17s (mean).
- If there was an auto tuning: 1s.
- If there was no auto tuning but an connection loss occurred: 0.65s.

3.2.3 The working process

No extraordinary error found during the experiment period.

3.3 Productivity calculations

Assume that the robot velocity is 1 m/s, the cycle time of the nut running process of each bike is about 10 seconds. That means that the productivity is 360 bikes per hour, in ideal condition.

Operation	**Time**
Robot moves to $\mathbf{P_{capture-i}}$	0.5s.
Calculate $\mathbf{P_{capture2-i}}$ and send to robot.	0.5s.
Robot moves to $\mathbf{P_{capture2-i}}$	0.5s.
Calculate $\mathbf{P_{hold}}$ and send to robot.:	0.5s.
Robot moves to $\mathbf{P_{hold-i}}$	0.2s.

Cylinder and robot moves $\mathbf{P_{run-i}}$.	1s.
Motor activated and tightening the nut.	4s.
Robot moves to the prepare position for the next station.	1s.
Cycle time (Added time for safety).	10s.

CHAPTER 4. CONCLUSION AND FUTURE WORK

4.1 Contributions

This thesis proposed a design of an automated nut running system for the back-wheel assembly of bicycles using robotic arm and computer vision. Its contributions include:

- An algorithm for estimating the nut-holding position based on the 2 images captured by the 2 cameras.
- A design of the robot tool and mounting cart.
- A design of the pneumatic and electric system.

The experiment shows that it can achieved productivity of 360 products per hour in ideal condition.

4.2 Future work

The future work includes increasing the accuracy of the algorithms, automating the current manually operated task and reduce the processing or signal transmission time.

BIBLIOGRAPHY

[1] S. Satoshi and A. Keiichi, "Topological structural analysis of digitized binary images by border following," *Computer Vision, Graphics, and Image Processing*, vol. 30, no. 1, p. 32–46, 1985.

[2] Zhang and Z., "A Flexible New Technique for Camera Calibration.," *IEEE Transactions on Pattern Analysis and Machine Intelligence.*, vol. 22, no. 11, pp. 1330-1334, 2000.

[3] Mark Nixon; Alberto Aguado, Feature Extraction and Image Processing for Computer Vision, London: Academic Press, 2019.

[4] Das Biman; Wang Yanqing, "Isometric Pull-Push Strengths in Workspace: 1. Strength Profiles," *International Journal of Occupational Safety and Ergonomics (JOSE)*, pp. Vol. 10, No. 1, 43–58, 2004.

[5] I. F. o. Robotics, "Executive Summary World Robotics 2019 Industrial Robots," [Online]. Available: https://ifr.org/downloads/press2018/Executive%20Summary%20WR%202019%20Industrial%20Robots.pdf. [Accessed 27 08 2020].

[6] Hadland Tony; Lessing Hans-Erhard, Bicycle Design_ An Illustrated History, London, England: The MIT Press, 2014.